Journal of Engineering Science and Technology
Vol. 12, No. 9 (2017) 2297 - 2314


# FUZZY FUSION OF PCA, ICA AND ILDA FACE ALGORITHMS FOR ENHANCED USER AUTHENTICATION

PRASHANT KUMAR JAIN*, SHAILJA SHUKLA, S. S. THAKUR

Jabalpur engineering College, Jabalpur, Madhya Pradesh, India
*Corresponding Author: pjain@jecjabalpur.ac.in

**Abstract**

Use of biometrics has increased over last few years due to its inherent advantages over customary identification tools such as token card and password, etc. In biometrics, after fingerprint, face recognition is second most preferred method with reasonably good accuracy. In some applications like CCTV cameras where face of a person is available for processing, face recognition techniques can to be very useful. In this paper, integration of face recognition techniques PCA, ICA and ILDA using fuzzy fusion method is detailed. The preliminary results clearly reveal that the fusion of methods improves the accuracy of the user identification.

Keywords: Face recognition, PCA, ICA, ILDA, Fuzzy logic.

## 1. Introduction

A biometric system which relies on a single biometric identifier is most of the time unable to meet the desired requirements in making a personal identification and verification. This happens due to the algorithm's limitations. Nowadays various biometric identifiers like, face, finger, voice, palm, retina and hand writing, etc., are used. However, each of these methods has its own advantages and disadvantages. This paper proposes a basic face recognition based system which is fuzzy fusion of principal component analysis (PCA), independent component analysis (ICA) and linear discriminant analysis (ILDA) algorithms.

## 2. Need for Biometrics

In the modern electronically/optically wired internet media and society, there are many circumstances (for example, making access of a multi-user computer account)

**Nomenclatures**

| | |
|---|---|
| A | Mixing matrix |
| C | Covariance matrix |
| $m$ | Mean value |
| $n_{ai}$ | Number of accepted impostor |
| $n_c$ | Number of all genuine identity claims |
| $n_{gi}$ | Number of images successfully assigned to the right identity |
| $n_i$ | Number of rejected genuine |
| $P_i$ | Pixel values |
| $S_i(t)$ | Source signal |
| $v_i$ | $i^{th}$coordinate of the facial image |
| $w_1$ | True identity |
| $w_2$ | False identity |
| $w_i$ | Mean centred image |
| $x(t)$ | Observed signal |
| $x_i$ | Class level |

***Greek Symbols***

| | |
|---|---|
| $\beta$ | Biometric System |
| $\varepsilon$ | Threshold |
| $\mu$ | Mean Value |
| $e_i$ | Eigen Vectors |
| $\lambda_i$ | Eigen Values |
| $\Omega_k$ | vector describing the$k^{th}$face class |
| $\Phi$ | Template |

**Abbreviations**

| | |
|---|---|
| AT&T | American Telephone & Telegraph |
| FAR | False Acceptance Rate |
| FRR | False Rejection Rate |
| ICA | Independent Component Analysis |
| LDA | Linear Discriminator Analysis |
| PCA | Principle Component Analysis |
| ROR | Rank-one recognition rate |

where a single person, as a user, needs to be verified by an electronic device. Generally, this verification of a user is based either on a certain token, for example, an ID card, something that can be possessed and/or the user has a particular knowledge such as password, something that is expected to be known only to the desired user. These approaches have various disadvantages. Tokens may be stolen, misplaced, lost, forged, or forgotten. Password may be forgotten or can be changed. In such a case system will not be able to differentiate between an authorized user and an imposter who has the "token" or "knowledge" of the authorized user. Hence, token knowledge-based authentication doesn't provide the sufficient security in critical application such as financial transactions. Therefore, to empower a biometric system to operate efficiently in different applications and situations, a multimodal biometric-system is preferred that works on the basis of multiple physiological or behavioural characteristics for the identification of a person. Considering a login based application on a network

which utilizes a biometric system for the identification of a user, in the event that a user is unable to provide good images of finger print (due of dry finger, cuts, etc.) the face and voice might be better biometric indicators. In the case of the "noisy" operating environment voice is not an appropriate biometric indicator. Further, if the "background" is cluttered, the face location algorithm, which is mandatory for face recognition, may not work in an efficient manner.

In this paper three basic algorithms PCA [1], ICA [2] and ILDA [3] are used for face recognition. In real time systems it is required that the user should be verified in few seconds, as he/she can't be keep waiting for minutes and hours. Moreover, accuracy should be high. Thus to increase accuracy complex algorithms are proposed but their processing time is more, therefore can't be easily used *n* real systems. Therefore in this paper, simple algorithms are considered to keep processing time less, but to raise accuracy more than one algorithms are used for user verification. The face and fingerprint results are combined together using the Fuzzy system, again fuzzy are used to minimize the processing time.

## 3. Problem Formulation

Face recognition is a process which investigates the similarity between the userface and the stored template to recognise the users identity.

Let $\beta$ denote a given biometric system, and let $\Phi^1, \Phi^2, \ldots\ldots\ldots \Phi^N$ are the template of the $N$ users which are enrolled in $\beta$, and have indicator number as $1, 2, \ldots\ldots\ldots N$. Each enrolled user has only one template. Let $\left(\Phi^0, I\right)$ denote the biometric indicator. The claimed identity, I, either belongs to category $w_1$ which indicates a true identity (a genuine user) or in $w_2$ which indicates the false identity (an imposter) (Fig. 1). The biometric system $\beta$ decides in favour of, $w_1$ or $w_2$ using the relation:

$$\mathrm{I} \in \begin{cases} w_1, & \text{if } F\left(\Phi^0, \Phi^1\right) > \varepsilon, \\ w_2, & \text{otherwise,} \end{cases} \tag{1}$$

where $F\left(\Phi^0, \Phi^1\right)$ is a function which measures the similarity between $\Phi^0$ and $\Phi^1$ and $\varepsilon$ is a threshold.

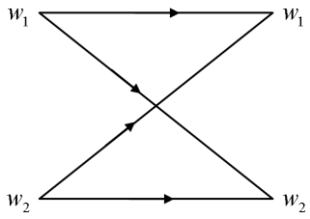


**Fig. 1.Binary nature of claim identity.**

For a claimed identity '*I*', there are four possibilities:

(i) a claimed identity in $w_1$ is determined to be in $w_1$,

(ii) a claimed identity in $w_1$ is determined to be in $w_2$,

(iii) a claimed identity in $w_2$ is determined to be in $w_2$,

(iv) a claimed identity in $w_2$ is determined to be in $w_1$.

Outcome (i) corresponds to a genuine user being accepted, outcome (ii) corresponds to a genuine user being rejected,outcome (iii) corresponds to an imposter user being rejected, and outcome (iv) corresponds to an imposter being accepted. Obviously, outcomes (i) and (iii) are correct whereas outcomes (ii) and (iv) are incorrect. Ideally, a biometric system should make only right decisions. In practise, because of the large intraclass variations in the acquired digital representation of the biometric indicator, incorrect decisions cannot be avoided. The performance measures of a biometric system are (i) false acceptance rate (FAR) and (ii) false reject rate (FRR). The FAR corresponds to the probability of outcome (iv) and the FRR is defined as the probability of outcome (ii). As the values of the FAR and FRR goes lower and lower, the reliability of the decision made by the system increases. The FAR and FRR values of a particular biometric system are determined by the inherent interclass and intraclass variations of the indicator and the design (e.g., feature extraction, decision making) of the system.

For the verification experiments, *ROC* curves, which plot the verification rate vs. false acceptance error (*FAR*). The FAR and FRR are defined as follows [1]:

$$FAR = \frac{n_{a_i}}{n_i} \times 100\%$$
$$FRR = \frac{n_{r_c}}{n_c} \times 100\% \quad (2)$$

where $n_{a_i}$ is the number of accepted impostor, $n_i$ is the number of all impostor identity claims made, $n_{r_c}$ is the number of rejected genuine, and $n_c$ is the number of all genuine identity claims made.

For the identification experiments, results are provided in the form of the rank-one recognition rate (*ROR*) is given by:

$$ROR = \frac{n_{g_i}}{n_g} \times 100 \quad (3)$$

where $n_{g_i}$ indicates the number of images successfully assigned to the right identity and $n_g$ is the overall number of images trying to assign an identity to.

## 4. Algorithms

In this section, three famous algorithms, principal component analysis, independent component analysis and linear discriminant analysis is presented.

### 4.1. Principal component analysis

A 2-D facial image can be represented as 1-D vector by concatenating each row (or column) into a long thin vector [2, 3]. Let us suppose we have *M* vectors of size *N* (= rows of image × columns of image) that represents a set of sampled images. If $p_j$ represents the pixel values then

$$x_i = [p_1, p_2 \ldots p_N]^T, \; i = 1 \ldots\ldots M \tag{4}$$

The images are made mean centered by the subtraction of the mean image from each image vector. Let $m = \frac{1}{M}\sum_{i=1}^{M} x_i$ represents the mean image, and let $w_i$ be defined as mean centred image

$$w_i = x_i - m \tag{5}$$

Our goal is to find a set of $e_i$'s which have the largest possible projection onto each of the $w_i$'s. We wish to find a set of *M* orthonormal vectors $e_i$ for which the quantity $\lambda_i = \frac{1}{M}\sum_{n=1}^{M}\left(e_i^T w_n\right)^2$ is maximized with the orthonormality constraint of

$$e_l^T e_k = \delta_{lk} \tag{6}$$

It has been shown that the $e_i$'s and $\lambda_i$'s are given by the eigenvectors and eigenvalues of the covariance matrix $C = WW^T$, where *W* is a matrix composed of the column vectors $w_i$ placed side by side [3]. The size of *C* is *N* × *N* which could be enormous. For example, images of size 64×64 create the covariance matrix of size 4096×4096. It is not practical to solve for the eigenvectors of *C* directly. According to a common theorem in linear algebra, the vectors $e_i$ and scalars $\lambda_i$ can be obtained by solving for the eigenvectors and eigenvalues of the *M*×*M* matrix $W^TW$. Let $d_i$ and $\mu_i$ be the eigenvectors and eigenvalues of $W^TW$ respectively. Therefore,

$$W^TWd_i = \mu_i d_i \tag{7}$$

By multiplying left to of both sides by *W*, we have

$$WW^TWd_i = W\mu_i d_i \tag{8}$$

which means that the first *M*-1 eigenvectors $e_i$ and eigenvalues $\lambda_i$ of $WW^T$ are given by $Wd_i$ and $\mu_i$ respectively. $Wd_i$ needs to be normalized in order to be equal to $e_i$. Since we only sum up a finite number of image vectors, $M$, the rank of the covariance matrix cannot exceed *M*-1 (The -1 come from the subtraction of the mean vector *m*).

The eigenvectors corresponding to nonzero eigenvalues of the covariance matrix produce an orthonormal basis for the subspace within which most image data can be represented with a small amount of error. The sorting of eigenvectors is done according to their corresponding eigenvalues from high to low. The eigenvector associated with the largest eigenvalue is one that reflects the greatest

variance in the image [3]. That is, the smallest eigenvalue is associated with the eigenvector that finds the least variance. They decrease in exponential fashion, meaning that the roughly 90% of the total variance is contained in the first 5% to 10% of the dimensions. A facial image can be projected onto $M' \square M$ dimensions by computing

$$\Omega = [v_1, v_2 ... v_M]^T \tag{9}$$

where $v_i = e_i^T w_i$. $v_i$ is the $i^{th}$ coordinate of the facial image in the new space, which came to be the principal component. The vectors $e_i$ are also images, so called, *eigenimages*, or *eigenfaces*[3]. They can be viewed as images and indeed look like faces. The simplest method for determining which face class provides the best description of an input facial image is to find the face class *k* that minimizes the Euclidean distance

$$\varepsilon_k = \|\Omega - \Omega_k\| \tag{10}$$

where, $\Omega_k$ is a vector describing the $k^{th}$ face class. If $\varepsilon_k$ is less than some predefined threshold, a face is classified as belonging to the class *k*.

### 4.1.1. Limitations of PCA

The main limitations of the PCA are as follows:

- The face image should be normalized and frontal-view.
- The system is an auto-associative memory system. It is harmful to be over-fitted.
- Training is very computationally intensive.
- It is hard to decide suitable thresholds.
- The suggested methods to deal with unknown faces and non-faces are not good enough to differentiate them from known faces.

### 4.1.2. Simulation results

Face images for the test are taken from AT&T data base. The database consists of 400 images. We have selected 12 images, for the demonstration of the algorithm. The files are in PGM format. Each image is displayed by 92×112 pixels, with 256 grey levels per pixel. The images are arranged in directories (one for each 'subject'), which have names of the form sX, where X indicates the subject number (between 1 and 40).

In the first case 12 images are taken as training set, each with mean 100 and standard deviation of 80. In the second step the mean and standard deviation of all images are changed for normalization. This is done to reduce the error due to lighting conditions and background.

The normalized images are shown in Fig. 3, and these images are very much similar to the images in Fig. 2, however when background changes abruptly, the normalization is very effective.

In the next step, the mean image is generated as shown in Fig. 4. The pixel values of the images ranges from 0 to 255.

In the next step, co-variance matrix is created, thereafter the Eigen-values are obtained, and the Eigen values close to zero are dropped and for the left over Eigen values, Eigen vector are obtained. Finally, after the normalization of Eigen vectors, Eigen faces are calculated as shown in Fig. 5.

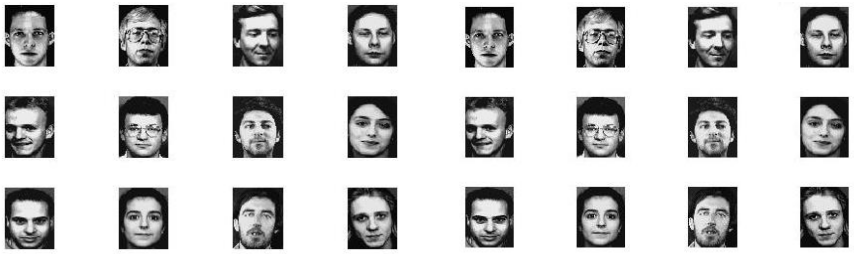

**Fig. 2. Training set (AT&T).**



**Fig. 3. Normalized training set (AT&T).**

**Fig. 4. Mean image.**

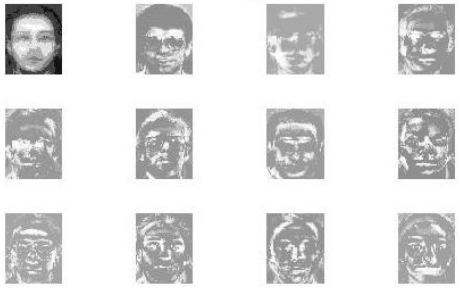

**Fig. 5.Eigenfaces.**

In case of user authentication, template matching is done. In Fig. 6, the input image and the re-constructed image are shown. The re-constructed image is very much similar to the input image.

**(a)**

**(b)**

**Fig. 6. (a) Input image. (b) Re-constructed image.**

Two pictures input and re-constructed images, deviate around the forehead portion, as the hair in input image is much more than in reconstructed image. Therefore, as in PCA only principal components are considered, therefore sometimes it may not be possible to exactly detect the input image.

## 4.2. Independent component analysis

Independent component analysis (ICA) is one of the most widely used Blind Source Separation (BSS) techniques for revealing hidden factors that underlie sets of random variables, measurements, or signals. Independent component analysis is essentially a method for extracting individual signals from the mixtures. Its power resides in the physical assumptions that the different physical processes generate unrelated signals.

The general model for ICA is that the sources are generated through a linear basis transformation, where presence of additive noise can be possible [4-6]. Suppose we have $N$ statistically independent signals, $s_i(t),\ i=1,2...,N$ . We assume that the sources themselves cannot be directly observed and that each signal, $s_i(t)$, is a realization of some fixed probability distribution at each time point $t$. Also, suppose $N$ sensors are being used for observing these signals, then we obtain a set of $N$ observation signals $x_i(t), i=1,2...,N$ that are mixtures of the sources. A basic and fundamental aspect of the mixing process is that the sensors must be spatially separated (e.g. microphones that are spatially distributed around a room) so that a different mixture of the sources is recorded by each sensor. We can model the mixing process with matrix multiplication as follows:

$$x(t) = As(t) \tag{11}$$

Where $A$ is an unknown matrix called the *mixing matrix* and $x(t)$, $s(t)$ are the two vectors representing the observed signals and source signals respectively. Incidentally, the justification for the description of this signal processing technique as *blind* is that we have no information on the mixing matrix, or even on the sources themselves. The objective is to recover the original signals, $s_i(t)$ from only the observed vector $x_i(t)$. We obtain estimates for the sources by first obtaining the "un-mixing matrix" $W$, where $W = A^{-1}$. This enables an estimate, $\hat{s}(t)$, of the independent sources obtained as

$$\hat{s}(t) = Wx(t) \tag{12}$$

The independent sources are mixed by the matrix A (which is unknown in this case). We seek to obtain a vector $y$ that approximates $s$ by estimating the un-mixing matrix $W$. In the case of accurate estimate of the un-mixing matrix, we obtain a good approximation of the sources.

The ICA model which is described above is the simple model since it ignores all noise components and any time delay in the recordings.

In ICA, same input training dataset is taken as in PCA to make comparison easier. The normalized dataset is presented in Fig. 7. For the above dataset the images of the Eigen faces is shown in Fig. 8. The input and the constructed images are shown in Fig. 9.

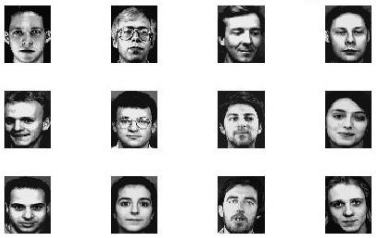

**Fig. 7. Normalized training database images (ICA).**

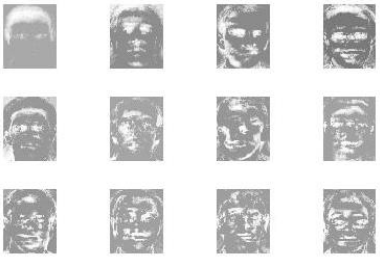

**Fig. 8. Eigenfaces(ICA).**

**(a)**

**(b)**

**Fig. 9. (a) Input image. (b) Re-constructed image.**

### 4.3. Linear discriminant analysis

LDA is a powerful face recognition technique that overcomes the limitation of PCA technique. The LDA maximizes the ratio of the determinant of the between-class scatter matrix to the determinant of the within class scatter matrix of the projected samples. Linear discriminant groups the images of the same class and separates the images of different classes of the images [4-8].

Considering a *C*-class problem with each class *i* consisting of a set of $N_i$ *d*-dimensional samples $\{x_1^i, x_2^i ... x_{N_i}^i\}$, where the superscript $(.)^i$ represents the class label. Define the total number of samples as $N = \sum_{i=1}^{C} N_i$, the probability of occurrence of class '*i*' as $p_i = \frac{N_i}{N}$, the sample mean for class '*i*' as $\mu^i = \frac{1}{N_i}\sum_{j=1}^{N_i} x_j^i$ and the grand sample mean as $\mu$ given by [1, 3]

$$\mu = \frac{1}{N}\sum_{i=j}^{C}\sum_{j=1}^{N_i} x_j^i = \sum_{i=j}^{C} P^i \mu^i \tag{13}$$

The within and between class scatter matrices represented as $\sum_W$ and $\sum_B$, respectively, and computed as

$$\sum_W = \sum_{i=1}^{C} P^i \sum_W^i = \frac{1}{N} \sum_{i=1}^{C} \sum_{j=1}^{N_i} \left(x_j^i - \mu^i\right)\left(x_j^i - \mu^i\right)^T$$
$$\sum_B = \sum_{i=1}^{C} P^i \sum_B^i = \frac{1}{N} \sum_{i=1}^{C} N_i \sum_{j=1}^{N_i} \left(\mu^i - \mu\right)\left(\mu^i - \mu\right)^T \quad (14)$$

In above expression, $\sum_w^i$ is the covariance matrix estimate for class *i* and is computed as

$$\sum_w^i = \frac{1}{N_i} = \sum_{j=1}^{N_i} \left(x_j^i - \mu^i\right)\left(x_j^i - \mu^i\right)^T \quad (15)$$

and $\sum_B^i$ is the scatter matrix between the class *i* and the 'grand class' and is computed as

$$\sum_B^i = \left(\mu^i - \mu\right)\left(\mu^i - \mu\right)^T \quad (16)$$

In other words, $\sum_W$ is estimated by 'pooling' together $\{\sum_w^i, i = 1...C\}$. Similarly, this also holds for $\sum_B$. Then, finally LDA evaluates a projection matrix *W*, say of size $r \times d$, that maximizes the criterion function [1, 3]

$$J_W = \frac{\det\left\{W^T \sum_B W\right\}}{\det\left\{W^T \sum_W W\right\}} \quad (17)$$

Above det{.} is matrix determinant. The maximum value of *r* is $d - 1$. For a test pattern *Y*, its class label $C_Y$ can be computed as

$$C_Y = \arg \min_{i=1,2,..C} \{W^T (y - \mu^i)^2 + D_i\} \quad (18)$$

where $D_i$ is used to incorporate prior information.

The AT&T lab database is used which consists of 40 folders. Each folder contains 10 images of a particular person with different facial expressions. The dataset is same as PCA, and the normalized dataset is presented in Fig. 10.

The fisher faces for the normalized training datasets are shown in Fig. 11. The mean image is shown in Fig. 12, which consists of feature of all the training images.

In Fig. 13, input and reconstructed images are shown. These images are very much similar, with slight difference in intensity.

**Fig. 10. Normalized training database images (ICA).**

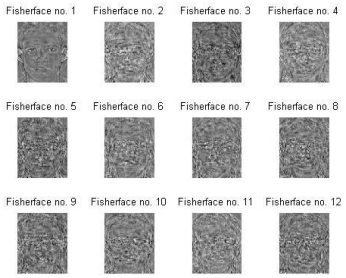


**Fig. 11. Fisherfaces (ICA).**

**Fig. 12.Mean images.**

**(a)**

**Fig. 13. (a) Input image.**

**(b)**

**(b) Re-constructed image.**

## 5. Results

In the section 5, results for different algorithms are presented, and in general they look similar to each other, thus different performance measures are developed to analyse the performance. The obtained results in terms of these measures are presented in this section. Results for above test are as follows:

For all simulations [9] only the first three images of each folder, i.e., 30% of the total images, as training images and rest 70% are used for verification.

In Table 1, the Rank one Recognition Rate for different methods using different number of Input images is shown. Form the table, it is clear that, as the total number of images is reduced the recognition rate increases. In case of PCA algorithm, for 100 images the recognition rate is 91.43% and for 400 images, it is 66.07%. Thus as the number of images is increased from 100 to 400, there is a large reduction in recognition rate. However, in case of ILDA algorithm, for 100 images the recognition rate is 95.71% and for 400 images, it is 86.07%. Thus the performance of ILDA algorithm is much better than the PCA algorithm. However, as the number of images is increased from 100 to 400 the performance of ILDA is not deteriorated much. The performance of the ICA algorithm lies between the PCA and ILDA algorithm. Therefore it can be concluded that for lesser number of images PCA can be easily chosen (simplest algorithm) while for larger number of images ILDA is the better option. But depending on the characteristic, there are some images which can be correctly recognized by a particular method only and since the three algorithms, in principle, are different, one of these can be applied depending on the application.

**Table 1. The rank one recognition rate for different methods using different number of input images.**

| Test Sample sizes (number of images) | PCA | ICA | ILDA |
|---|---|---|---|
| 400 (280+120) | 66.07% | 75.83% | 86.07% |
| 300 (210+90) | 70.48% | 80.56% | 90.48% |
| 200 (140+60) | 79.29% | 86.31% | 93.57% |
| 100 (70+30) | 91.43% | 93.26% | 95.71% |

In Table 2, the equal error rate for different methods using different number of input images is shown. In case of PCA algorithm, for 100 images the equal error rate is 1.43% and for 400 images, it is 5.03%. Thus as the number of images is increased from 100 to 400, the equal error rate increases. However, in case of ICA algorithm, for 100 images the equal error rate is 1.43% and for 400 images, it is 4.78%, and similarly for ILDA, it increases from 1.43% for 100 images to 4.28% for 400 images. Thus, again the performance of ILDA algorithm is better than the PCA and ICA algorithm. But again for lesser number of images equal error rate is same for all the three algorithms. The performance of the ICA algorithm lies between the PCA and ILDA algorithm.

**Table 2. The equal error rate for different methods using different number of Input images.**

| Test Sample sizes (number of images) | PCA | ICA | ILDA |
|---|---|---|---|
| 400 (280+120) | 5.03% | 4.78% | 4.28% |
| 300 (210+90) | 3.40% | 3.36% | 3.33% |
| 200 (140+60) | 2.86% | 2.51% | 2.26% |
| 100 (70+30) | 1.43% | 1.43% | 1.43% |

In Table 3, the verification rate at 1% FAR for different methods using different number of input images is shown. For 100 images the verification rate at 1% FAR is 98.57% for all the three methods. It is also observable form the table that, as the number of images is increased from 100 to 400, the verification at 1% FAR rate increases. However, in case of ILDA algorithm, for 400 images the verification rate at 1% FAR is very impressive of 90.0%. Thus, again the performance of ILDA algorithm is better than the PCA and ICA algorithm. For 200 or less images the performance of all the three algorithms in terms of verification rate at 1% FAR is almost the same.

**Table 3. The verification rate at 1% FAR rate for different methods using different number of Input images.**

| Test Sample sizes (number of images) | PCA | ICA | ILDA |
|---|---|---|---|
| 400 (280+120) | 86.79% | 88.56% | 90.00% |
| 300 (210+90) | 87.14% | 89.87% | 92.86% |
| 200 (140+60) | 95.71% | 95.54% | 95.00% |
| 100 (70+30) | 98.57% | 98.57% | 98.57% |

In Table 4, the performance of different algorithms for different metric for 400 images is tabulated. The equal error rate for PCA, ICA and ILDA is 5.03%, 4.87% and 4.28% respectively. The verification rate at 1% FAR is 90.00% of

ILDA and decreases down to 64.29% for verification rate at 0.01% FAR. Thus, as the false acceptance rate decreases the percentage of verification reduces significantly. Now, even in case of ILDA algorithm, at 0.01% FAR the verification rate is poor. In comparison, the performance of ILDA algorithm is better than the PCA and ICA algorithm but not acceptable. Therefore in security prone areas these methods alone cannot provide robust solution.

**Table 4. Performance of different algorithms for different metric for 400 images.**

| Test Sample sizes (number of images) | PCA | ICA | ILDA |
|---|---|---|---|
| The equal error rate | 5.03% | 4.87% | 4.28% |
| The verification rate at 1% FAR | 86.79% | 88.56% | 90.00% |
| The verification rate at 0.1% FAR | 66.79% | 70.48% | 76.43% |
| The verification rate at 0.01% FAR | 45.00% | 56.17% | 64.29% |

In Fig. 14, the verification rate vs. false acceptance rate is plotted for PCA. As obvious as the false acceptance rate increases the verification rate increases. It must be remembered that as the overall verification rate increases the falsely accepted images also increases. Thus, in the applications were very low false acceptance rate is desired PCA fails. The figure also depicts that as the number of training images increasers from 2 to 4, the verification rates also improves by a factor of 10. Therefore, more number of images is required for the correct verification.

In Fig.16, the verification rate vs. false acceptance rate is plotted for ICA with varying number of total images. Again as the false acceptance rate increases the verification rate increases. Four curves for a total of 100, 200, 300 and 400 images are shown in the figure. It is clear from the figure that as the total number of images increases the verification rate decreases. By comparing Figs. 15 and 16, it can be seen that the performance of the ICA algorithm is better in comparison to PCA algorithm.

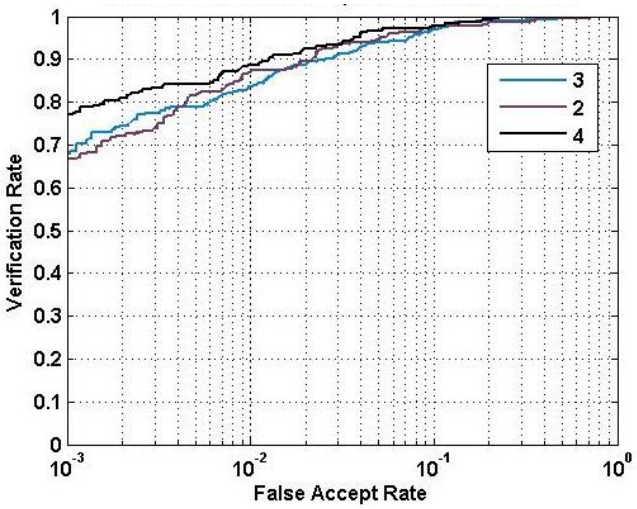


**Fig. 14.ROC curve for PCA for different number of training images (ORL database).**

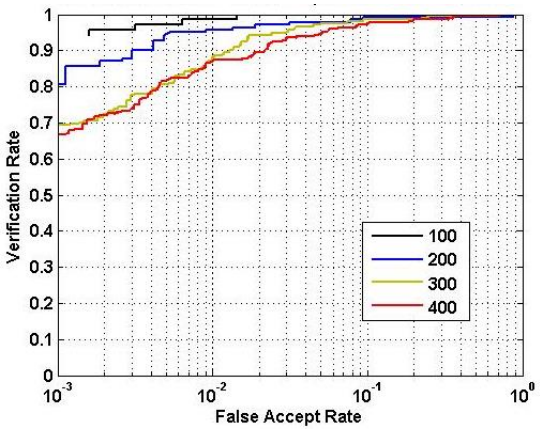


**Fig. 15. ROC curve for PCA for different number of images (ORL database).**

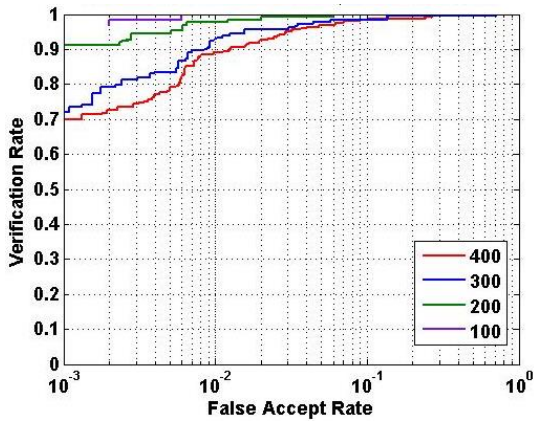


**Fig. 16.ROC curve for ICA for different number of images (ORL database).**

In Fig.17, the verification rate vs. false acceptance rate is plotted for ILDA with varying number of total images. For the false acceptance rate of 10% the verification rate is nearly 100%.

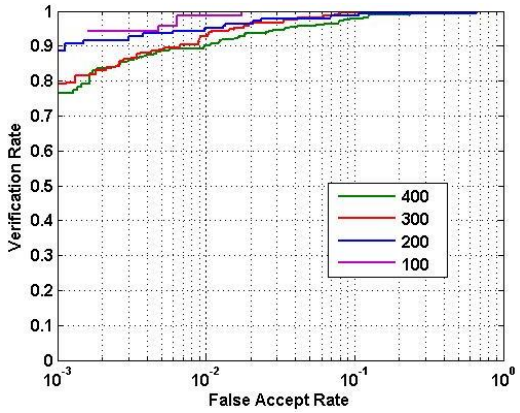


**Fig. 17.ROC curve for ILDA for different number of images (ORL database).**

But such a high false acceptance rate is not acceptable. It can be seen from the figure that the verification rate is above 90% for false acceptance rate of 1%. By comparing Figs. 15, 16, and 17 it is clear that the performance of the ILDA algorithm is better in comparison to PCA and ICA algorithm.

## 6. Fuzzification of Face Recognition Method

The Fuzzification of the Face recognition techniques is shown in Fig. 18. Here, the results of the PCA, ICA, and ILDA are fuzzified to obtain more accurate identification [10-13]. For the input of the Fuzzifier the selected membership function is $\prod$ and at the output of the fuzzy system the membership function is chosen to be $\Delta$.

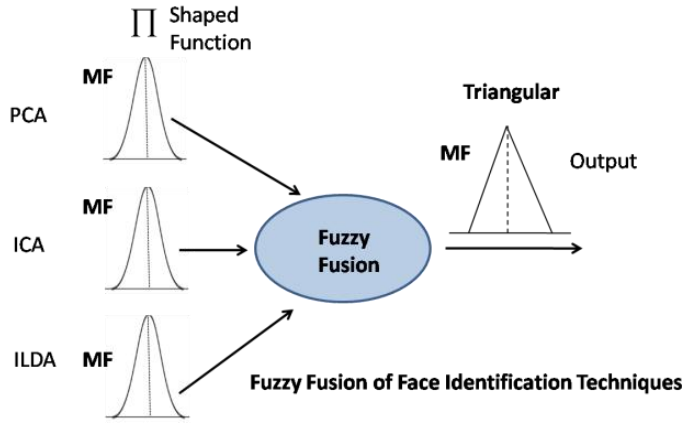


**Fig. 18. Fuzzy fusion of PCA, ICA and ILDA.**

In the input function $\Pi$, the parameters $\alpha, \beta$ and $\gamma$ define the minimum, maximum and mean value of the training data set, respectively. The constants $c_1$, $c_2$ define the 0.5 value of the membership function.

$$\Pi(z;\alpha,\gamma,\beta)=\begin{cases}0 & z\le\alpha\\ 2^{m-1}\left(\dfrac{z-\alpha}{\gamma-\alpha}\right)^m & \alpha<z\le c_1\\ 1-2^{m-1}\left(\dfrac{\gamma-z}{\gamma-\alpha}\right)^m & c_1<z\le\gamma\\ 2^{m-1}\left(\dfrac{z-\gamma}{\beta-\gamma}\right)^m & \gamma<z\le c_2\\ 1-2^{m-1}\left(\dfrac{\beta-z}{\beta-\gamma}\right)^m & c_2<z\le\beta\\ 0 & z\ge\beta\end{cases} \tag{19}$$

The value of the *m* can be selected to alter the shape of the $\Pi$ function. In this work the value of *m* is taken to be 2.

It is observable from Fig.19 that the shape and structure of the $\Pi$ function can be altered by varying the mentioned parameters.

Figure 20, shows the face recognition rate for PCA, ICA, ILDA and for the fusion of these three processes. As discussed previously the PCA method is poorest, and the performance of the ILDA is much better in comparison to other discussed methods. Again in this case, as the FAR increases, the recognition rate increases. However as the large FAR is not acceptable in most of the applications, therefore all the above three methods are combined using fuzzy methods and the obtained results are superior in comparison to others. However, again the recognition rate is not very good at low FAR.

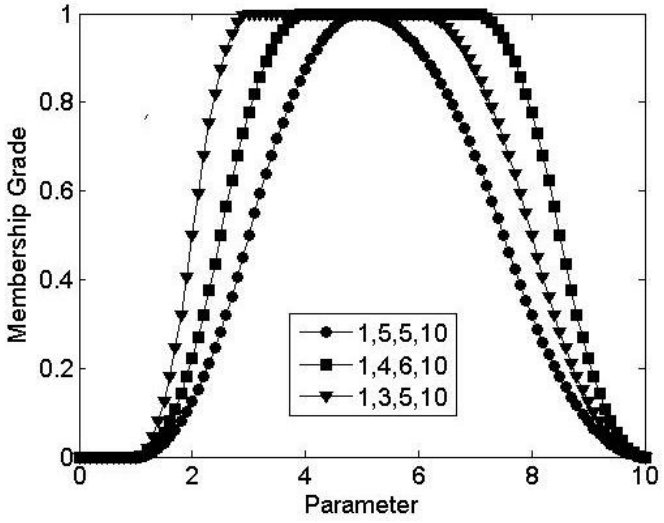


**Fig. 19.The $\Pi$ membership function.**

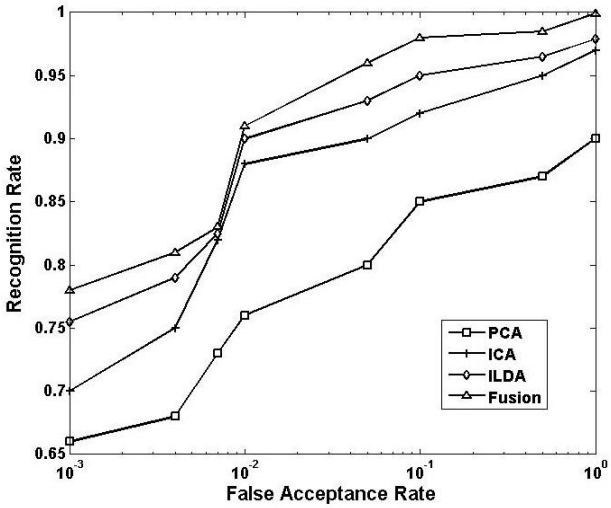


**Fig. 20. FAR vs. Recognition rate for Face matching algorithms.**

## 7. Conclusions

In this paper, three face recognition algorithms PCA, ICA and ILDA are discussed. These algorithms are not the most accurate of face recognition techniques but definitely are one of the easiest to implement. Due to time restrictions in real time systems, these methods were adopted over more accurate methods. The face recognition program returned good results with a few discrepancies. The eigenvalues and eigenvectors of a group of images were calculated correctly. Faces were able to be compared correctly using their decomposition coefficients. Faces were successfully verified as user faces and then the corresponding user was successfully logged on. The comparison of these algorithms is done in terms for performance metrics equal error rate, verification rate at 1, 0.1, 0.01% FAR, etc. Overall the performance of ILDA is much better than other two algorithms. Even for the ILDA algorithm, the verification rate at 0.01% FAR is 64.29% which is well below acceptable limits. In security applications where 99.999% accuracy is needed, these method in alone cannot be used. Thus to enhance accuracy more than one technique is needed.

## References

1. Delac, K.; Grgic, M.; and Grgic, S. (2006). Independent comparative study of PCA, ICA, and LDA on the FERET data set. *International Journal of Imaging Systems and Technology*, 15(5), 252-260.
2. Hyvarinen, A.; Karhunen J.; and Oja, E (2001). Independent Component Analysis. Wiley, New York.
3. Beveridge, J.R.; She, K.; Draper, B.A.; and Givens, G.H. (2001). A nonparametric statistical comparison of principal component and linear discriminant subspaces for face recognition, *Proceedings of the IEEE Conference on ComputerVision and Pattern Recognition*, 1(1), 535-542.
4. Bellhumer, P.N.; Hespanha, J.; and Kriegman, D. (1997). Eigenfaces vs. fisherfaces: Recognition using class specific linear projection. *IEEE Transactions on Pattern Analysis and Machine Intelligence*, 19(7), 711-720.
5. Slavković, M.; and Jevtić, D. (2012). Face recognition using eigenface approach. *Serbian Journal of Electrical Engineering*. 9(1), 121-130.
6. Bartlett, M.S.; Movellan, J.R.; and Sejnowski, T.J. (2002). Face recognition by independent component analysis, *IEEE Transaction on Neural Networks*, 13(6), 1450-1464.
7. Yambor, W.S.; Draper, B.; and Beveridge, J.R. (2002). Analysing PCA-based face recognition algorithms: eigenvector selection and distance measures, *Empirical Evaluation Methods in Computer Vision*, World Scientific Press, Singapore, 1-15.
8. Zhao, W.; Chellastra, R.; Rosenfeld, A.; and Phillips, P.J. (2003). Face recognition: a literature survey, *ACM Computing Surveys*, 35(4), 399-458.
9. Riley, (1981). Expert Systems - Principle and programming (Pws-Kent, Boston, 1-59.
10. Kwak K.C.; and Pedrycz, W. (2005). Face recognition: A study in information fusion using fuzzy integral. *Pattern Recognition Letters*. 26(12), 719-733.

11. Dass S. C.; Nandakumar, K.; and Jain, A.K. (2005). A principal approach to score level fusion in multimodal biometrics system. *P*roceedings of ABVPA
12. .Jain, P.; Shukla, S.; and Thakur, S.S. (2014). User authentication using multimodel finger-print recognition. *International Journal of Computer Science and Information Technologies*, 5 (2), 2596-2603.
13. Jain, P.; Shukla, S.; and Thakur, S.S. (2014). User authentication using multimodel face recognition. *International Journal of Applied Engineering Research*, 9(20), 6559-6570.